International Journal of Mass Spectrometry 280 (2009) 184–189

Contents lists available at ScienceDirect

International Journal of Mass Spectrometry

journal homepage: www.elsevier.com/locate/ijms

Size-dependent reactivity of cobalt cluster ions with nitrogen monoxide: Competition between chemisorption and decomposition of NO

Tetsu Hanmura[a,1], Masahiko Ichihashi[b], Ryuji Okawa[c,2], Tamotsu Kondow[b,*]

[a] East Tokyo Laboratory, Genesis Research Institute, Inc., 717-86 Futamata, Ichikawa, Chiba 272-0001, Japan
[b] Cluster Research Laboratory, Toyota Technological Institute: in East Tokyo Laboratory, Genesis Research Institute, Inc., 717-86 Futamata, Ichikawa, Chiba 272-0001, Japan
[c] Department of Applied Chemistry, Graduate School of Science and Engineering, Chuo University, 1-13-27 Kasuga, Bunkyo-ku, Tokyo 112-8551, Japan

ARTICLE INFO

Article history:
Received 14 July 2008
Received in revised form 19 August 2008
Accepted 23 August 2008
Available online 5 September 2008

Keywords:
Cobalt cluster ion
Nitrogen monoxide
Chemisorption
Decomposition

ABSTRACT

Reactions of NO molecules on cobalt cluster ions were studied in a beam-gas geometry by using a tandem mass spectrometer. Single-particle collision reactions of Co_mNO^+ ($m = 3$–10) with NO were found to proceed in such a manner that NO decomposition dominates at $m = 4$–6 with the maximum reaction cross section at $m = 5$ and chemisorption dominates in $m \geq 7$. On the other hand, in two-particle collision reactions of Co_n^+ ($n = 2$–10) with NO, NO decomposition at $n \geq 5$ and chemisorption of two NO molecules with Co atoms loss at $n \geq 8$ were found to proceed. These results indicate that the size-dependency of the multiple collision reactions originates from secondary attacking of an NO molecule to primary products of the initial single collision reactions. The DFT calculation supports the scheme that both the decomposition and chemisorption of two-particle collision reactions proceed via a common intermediate, $Co_mN_2O_2^+$, in which the two NO molecules are dissociatively chemisorbed on the cobalt cluster ion, and the size-dependency of the two-particle collision reactions is explained in terms of the structure of this reaction intermediate.

1. Introduction

It is well recognized in heterogeneous catalysis that the catalytic activity changes with the diameter (nanometer or larger) of the supported catalytic particles such as metal particles [1], probably because the surface structure (morphology) and the electronic structures change with the diameter [2]. Even particles having nanometers in diameters show properties expected on the extension of their bulk properties whereas particles (clusters) having sub-nanometers in diameters exhibit totally different properties from those of the bulk [3]. Namely, it is expected that clusters have catalytic reactivity which is scarcely encountered in traditional catalysis. From this viewpoint, several attempts have been made so far in spite of the difficulty of preparing size-selected clusters free of any effects due to adjacent surface atoms, etc.; in a cluster regime, the reactivity of clusters changes sensitively with the number of the constituent atoms (cluster size) and environments such as a surface in contact with the cluster.

Let us consider metal clusters in particular hereafter. In order to elucidate the fundamental properties of the metal clusters, size-selected free metal clusters should be prepared in the gas phase so that one can eliminate the effects due to their environments. In addition, the separation of the environmental effects from the overall properties facilitates the design of catalysis if one desires to use the information for the design [4–6]. Note that clusters having any desired size are prepared in the gas phase and are free from any effect due to their environments; they show the size-specific reactivity and selectivity, that is, the reaction products and the rate change with their size. Drastic size-dependency is expected in a smaller size range because both the geometric and the electronic structures of the clusters are affected significantly by addition or removal of one atom [7].

Among many kinds of trace species present in the atmosphere, nitrogen monoxide, NO, attracts much attention because (1) NO is one of the common species in the emissions from industrial activities, (2) NO itself is an air pollutant which is harmful to

* Corresponding author. Tel.: +81 47 320 5911; fax: +81 47 327 8031.
E-mail address: kondow@clusterlab.jp (T. Kondow).
[1] Present affiliation: Fujikura Ltd.
[2] Present affiliation: Nippon Paint Co., Ltd.

1387-3806/$ – see front matter © 2008 Elsevier B.V. All rights reserved.
doi:10.1016/j.ijms.2008.08.024

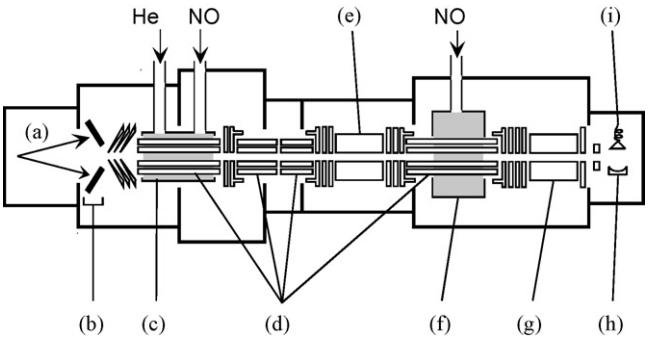

Fig. 1. Schematic drawing of the apparatus employed; (a) xenon ion beam, (b) cobalt metal plates, (c) cooling cell, (d) octopole ion guides, (e) first quadrupole mass filter, (f) reaction cell, (g) second quadrupole mass filter, (h) ion conversion dynode, and (i) secondary electron multiplier.

animals and plants, and (3) NO indirectly affects the balance of other important trace species such as ozone because NO participates in the cycles of the reactions occurring in the atmosphere [8]. Therefore, the catalytic decomposition of NO by metal clusters has both the fundamental and the practical importance. In this connection, reactions of NO on metal cluster ions, Co_n^+ [9], Ni_n^+ [10], $Nb_n^{+/-}$ [11], and $Rh_n^{+/-}$ [12,13], have been investigated, and these studies indicate the critical importance of dissociative chemisorption in the catalytic removal of NO. Among these metals, cobalt is one of the materials whose reactivity toward NO receives much attention because Co_3O_4 is known to catalyze the direct decomposition of NO [14,15]. So far, Klaassen and Jacobson [16,17] have observed reactions of $^{18}O_2$ and $H_2{}^{18}O$ with $Co_n(N^{16}O)^+$ (n = 2–4) in FT-ICR, and have concluded that NO is molecularly chemisorbed on Co_2^+ while dissociatively chemisorbed on $Co_{3,4}^+$. This finding is supported by the theoretical study by Salahub and co-workers [18].

In the previous study [19], we have observed the reactions of NO with cobalt cluster ions, Co_n^+ (n = 2–10), under single collision conditions and found that the NO molecule is efficiently chemisorbed on Co_n^+, probably dissociatively, giving $Co_{n-1}NO^+$ in the size range of $n \geq 4$. In the course of the actual NO removal, the chemisorbed NO molecule must further interact with other NO molecules. In the present report, we studied the reactions of Co_mNO^+ (m = 3–10) with NO molecules under single collision conditions in order to scrutinize the reaction mechanisms of the collisional reactions of NO molecules with Co_n^+ (n = 2–10) under multiple collision conditions. The reaction processes and the energetics were analyzed with the aid of the DFT calculation. Mackenzie and co-workers have studied reactions involving sequential collisions between cobalt cluster ions and NO molecules in FT-ICR and derived complimentary information[3] on the mechanism.

2. Experimental

Fig. 1 shows a schematic diagram of the apparatus used in the present study. Only the modification made for the present study is closely described here, since its detail has been given elsewhere [20,21]. The apparatus consists of an ion source, a cooling cell, quadrupole mass filters, a reaction cell, and a detector, which are connected by octopole ion guides.

[3] Private communication, Doctoral dissertation of M. Anderson, University of Warwick, 2007.

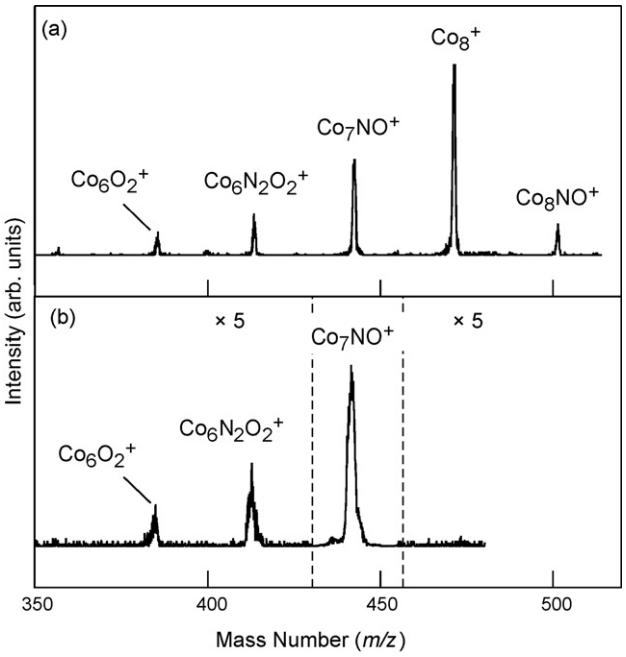

Fig. 2. Mass spectra obtained in the reaction of Co_8^+ with NO under a multiple collision condition (panel (a)), and in the reaction of Co_7NO^+ with NO at the collision energy of 0.2 eV under a single collision condition (panel (b)). The peaks assigned to the product ions in panel (b) are vertically enlarged by 5 times.

The cluster ions, Co_n^+, were produced by an ion-sputtering technique in which gaseous xenon is ionized in the discharge ion source (Rokion Ionenstrahl-Technologie, CORDIS Ar25/35c), accelerated at the energy of 13 keV, and then irradiated onto four targets of Co metal. The cluster ions thus produced were extracted by ion optics and cooled down to the room temperature by more than 100 collisions with He atoms in the cooling cell; the pressure of the He gas was kept at $>10^{-3}$ Torr. Then, Co_n^+ were size-selected in the first quadrupole mass filter (Extrel, 162–8), and admitted into the octopole ion guide located in the center of the reaction cell in which the incoming cluster ions react with NO molecules. The NO pressure in the reaction cell was monitored by a spinning rotor gauge (MKS, SRG–2) and regulated in the range of 10^{-5}–10^{-4} Torr by a variable leak valve (Granville-Phillips, Series 203). Both the single and the multiple collision conditions were realized by adjusting the NO pressure in this pressure range. The product ions out of the reaction cell were mass-analyzed by the second quadrupole mass filter (Extrel, 162–8) and detected by the combination of an ion conversion dynode and a secondary electron multiplier (Burle, Channeltron 4139S) in the pulse counting mode.

In the reactions of Co_mNO^+, the parent cluster ion, Co_mNO^+, was prepared by the adsorption of an NO molecule onto Co_n^+ in the cooling cell. A small amount of NO gas was introduced into the cooling cell with a partial pressure of $\approx 10^{-5}$ Torr. The partial pressure of He was much higher than that of NO, so that the internal temperature of Co_mNO^+ produced was cooled down to the room temperature by the collisions with the He atoms. Then, Co_mNO^+ was mass-selected and admitted to react with another NO molecule as described above.

The collision energy in the single collision reaction was determined from the translational energy of the parent ion in the reaction cell. The translational energy was controlled by varying the dc bias of the octopole ion guide at the reaction cell. The spread of the translational energy was measured to be typically 3 eV in the laboratory frame by applying a retarding voltage to the ion guide.

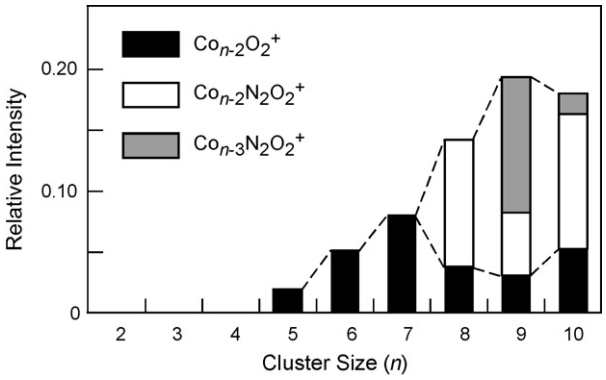

Fig. 3. Relative intensities of the product ions with respect to the total ion intensity for the multiple collision reactions of Co_n^+ with NO at the NO pressure of 3×10^{-4} Torr.

For example, this energy spread makes the uncertainty (±0.1 eV) of the collision energy in the center-of-mass frame in a collision involving Co_6^+.

Total and partial reaction cross sections for a single collision reaction were determined from the measured ion intensities. The total reaction cross section, σ_r, for obtaining any reaction product ion is given as

$$\sigma_r = \frac{k_B T}{Pl} \ln \frac{I + \Sigma I_p}{I}, \quad (1)$$

where I and $\sum I_p$ represent the intensity of the intact parent ion passing through the collision region and the sum of the intensities of the product ions, respectively, P and T are the pressure and the temperature of NO gas in the reaction cell, respectively, l (=120 mm) is the effective path length of the collision region, and k_B is the Boltzmann constant. The partial reaction cross section, σ_p, for the formation of each product ion is expressed as

$$\sigma_p = \sigma_r \frac{I_p}{\Sigma I_p}, \quad (2)$$

where $I_p/\sum I_p$ represents the branching fraction for the product ion of interest. The uncertainty of the reaction cross sections arises from (1) systematic errors caused by the uncertainties in the ion collection efficiency and in determining P and l, and (2) statistical errors caused by the fluctuation of the ion intensity. The systematic and the statistical errors are typically 30% and 10%, respectively. The systematic errors are ignorable when the size- and collision-energy dependence of the reaction cross sections are interested.

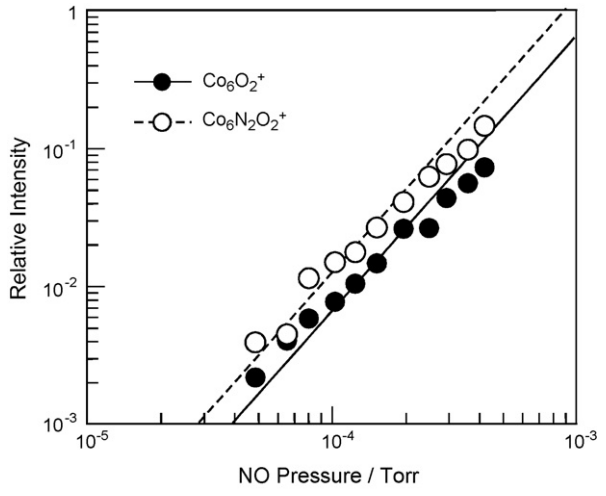

Fig. 4. Relative intensities of the product ions, $Co_6O_2^+$ (●) and $Co_6N_2O_2^+$ (○), by the multiple collision reactions of Co_8^+ with NO are plotted as a function of the NO pressure in the reaction cell. The solid and broken lines are eye-guides showing the slope proportional to the square of the NO pressure.

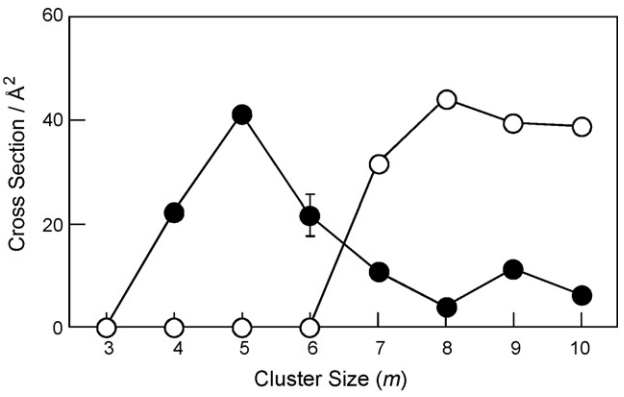

Fig. 5. Reaction cross sections for the production of $Co_{m-1}O_2^+$ (●) and $Co_{m-x}N_2O_2^+$ (x = 1, 2) (○) by the single collision reactions of Co_mNO^+ with NO at the collision energy of 0.2 eV are plotted as a function of the cluster size. The error bar gives one-standard deviation of the statistical errors due to fluctuation of the ion intensities.

3. Results

Fig. 2(a) shows a typical mass spectrum of Co_8^+ with NO under a multiple collision condition. Among the product ions observed in the mass spectrum, Co_7NO^+ and Co_8NO^+ are likely to be produced through a single collision reaction between Co_8^+ and an NO molecule because the same product ions are observed in the reaction of Co_n^+ with an NO molecule [19]. The other product ions, $Co_6O_2^+$ and $Co_6N_2O_2^+$, are produced by multiple collision reactions because at least two NO molecules are necessary to produce O_2 or N_2O_2 of these product ions. The reactions giving $Co_{n-2}O_2^+$ and $Co_{n-x}N_2O_2^+$ (x = 2, 3) are defined as NO decomposition and chemisorption of two NO, respectively. Fig. 3 shows the relative intensities of the product ions at the NO pressure of 3×10^{-4} Torr in the reaction cell, where the intensities are normalized against the total intensity of ions including the intact parent ion. The product ions, $Co_{n-2}O_2^+$ and $Co_{n-x}N_2O_2^+$, start to be observed at n = 5 and n = 8, respectively. Note that Fig. 3 gives only a rough picture for the size-dependence of the reactivity since the product ion intensity of the multiple collision reactions changes with the NO pressure. Fig. 4 shows the relative intensities of $Co_6O_2^+$ and $Co_6N_2O_2^+$ in the reactions of Co_8^+ with NO as a function of the NO pressure in the reaction cell. The intensity of each product ion increases in proportion to the square of the NO pressure.

Fig. 2(b) shows a typical mass spectrum obtained by the reactions of Co_7NO^+ with NO under a single collision condition. The parent cluster ion, Co_8^+, reacts with NO molecules to generate $Co_6O_2^+$ and $Co_6N_2O_2^+$ under the multiple collision conditions (see Fig. 2(a)), while Co_7NO^+ gives the same product ions under the single collision conditions. Fig. 5 shows the size-dependence of the partial cross sections of Co_mNO^+, from which $Co_{m-1}O_2^+$ and $Co_{m-x}N_2O_2^+$ (x = 1, 2) are generated, at the collision energy of 0.2 eV. The production of $Co_{m-1}O_2^+$ occurs only at m = 4–6, while that of $Co_{m-x}N_2O_2^+$ dominates at $m \geq 7$. This finding shows that there exists a clear connection between the threshold sizes for the reactions of Co_mNO^+ and Co_n^+; the NO decomposition and the chemisorption of two NO start to be detected at the threshold sizes of m = 4 and 7, respectively, for Co_mNO^+, while at the threshold sizes of n = 5 and 8, respectively, for Co_n^+. The threshold sizes for Co_n^+ are larger by one than those for Co_mNO^+.

4. Discussion

4.1. Double collision reactions

A number of NO molecules involved in the reactions of Co_n^+ can be determined from the dependence of the product ion intensities on an NO pressure in the reaction cell. Indeed, it was proved that the double collision reactions involving two NO molecules give the product ions, $Co_{n-2}O_2^+$ and $Co_{n-x}N_2O_2^+$, because the product ion intensities increase proportionally with the square of the NO pressure as shown in Fig. 4.

This finding, together with the fact that $Co_{n-1}NO^+$ is the dominant product ion in the single collision reaction of Co_n^+ with NO [19], leads us to conclude that two NO molecules sequentially react with Co_n^+ under the multiple collision conditions as follows:

$$Co_n^+ + NO \rightarrow Co_{n-1}NO^+ + Co \quad (3)$$

$$Co_{n-1}NO^+ + NO \rightarrow Co_{n-2}O_2^+ + CoN_2 \quad (4)$$

$$Co_{n-1}NO^+ + NO \rightarrow Co_{n-1-x}N_2O_2^+ + xCo \quad (x = 1, 2) \quad (5)$$

At first Co_n^+ reacts with an NO molecule and gives $Co_{n-1}NO^+$ (Eq. (3)). Another NO molecule reacts with $Co_{n-1}NO^+$ and then the final products are formed (Eqs. (4) and (5)). Similar reaction processes have been proposed for the reaction between Rh_n^+ and NO molecules [13]. As shown in Fig. 3, the production of $Co_{n-2}O_2^+$ and $Co_{n-x}N_2O_2^+$ ($x = 2, 3$) from Co_n^+ depends on the cluster size significantly. This size specificity is likely to originate from the processes involving the second NO molecule (Eqs. (4) and (5)), since the reaction cross section of the first process (Eq. (3)) at $n \geq 4$ is almost independent of the cluster size [19] and is comparable to the collision cross section approximated by the Langevin cross section [22].

In order to confirm the mechanism proposed here, the intermediate ion, Co_mNO^+, was prepared and allowed to react with NO. This reaction is expected to simulate the reaction between $Co_{n-1}NO^+$ and NO (Eqs. (4) and (5)) in the double collision reactions as shown in the following section.

4.2. $Co_mNO^+ + NO$

4.2.1. Reaction processes involving second NO molecule

The reaction products from Co_mNO^+ (see Fig. 2(b)) are made by the reactions identical to Eqs. (4) and (5). The NO molecule in Co_mNO^+ is dissociatively chemisorbed as $Co_m(N)(O)^+$ [19]. The reactions of $Co_m(N)(O)^+$ and NO are assumed to proceed via the following steps:

$$Co_m(N)(O)^+ + NO \rightarrow Co_m(N)(O)(NO)^+ \quad \text{(molecular chemisorption)} \quad (6)$$

$$Co_m(N)(O)(NO)^+ \rightarrow Co_m(N)_2(O)_2^+ \quad \text{(dissociative chemisorption)} \quad (7)$$

$$Co_m(N)_2(O)_2^+ \rightarrow Co_m(N_2)(O)_2^+ \quad \text{(formation of } N_2\text{)} \quad (8)$$

$$Co_m(N_2)(O)_2^+ \rightarrow Co_{m-1}(O)_2^+ + CoN_2 \quad (9)$$

$$Co_m(N)_2(O)_2^+ \rightarrow Co_{m-x}(N)_2(O)_2^+ + xCo \quad (10)$$

At first, the second NO molecule which collides with $Co_m(N)(O)^+$ is molecularly chemisorbed (Eq. (6)), and then dissociates into atomic N and O on the cluster (Eq. (7)). Since the intermediate species, $Co_m(N)_2(O)_2^+$, is isolated in the vacuum, the chemisorption energy of the second NO is retained in $Co_m(N)_2(O)_2^+$. Therefore, $Co_m(N)_2(O)_2^+$ has a large internal energy and cannot survive without dissociation during the flight time from the reaction cell to the detector (~100 μs). Both the detected products, $Co_{m-1}(O)_2^+$ and $Co_{m-x}(N)_2(O)_2^+$, are likely to be formed via this common intermediate species, $Co_m(N)_2(O)_2^+$. In the course of the production of $Co_{m-1}(O)_2^+$ (the NO decomposition), two N atoms interact with each other on the cluster to form the molecular N_2 (Eq. (8)), and then the intermediate species, $Co_m(N_2)(O)_2^+$, releases CoN_2 to form $Co_{m-1}(O)_2^+$ (Eq. (9)), although the neutral product, CoN_2, released is not detectable in the present experiment. The release of CoN_2 is energetically more likely than that of Co and N_2; in fact the binding energy of Co–N_2 amounts to ~2 eV by a DFT calculation [23]. On the other hand, in the course of the production of $Co_{m-x}N_2O_2^+$ (the chemisorption of two NO), one or two Co atoms are released from the common intermediate species, $Co_m(N)_2(O)_2^+$ (Eq. (10)).

As shown in Fig. 5, the reaction cross section of Co_mNO^+ with NO shows characteristic size-dependency which is summarized as follows:

(1) No reaction occurs on smaller clusters of $m \leq 3$,
(2) only the NO decomposition occurs at $m = 4$–6, while the chemisorption of two NO dominates in $m \geq 7$, and
(3) the NO decomposition at $m = 5$ and the chemisorption of two NO at $m = 7$–9 proceed near the collision limit because the reaction cross sections at these sizes are close to the Langevin cross section (=49.3 Å^2 at the collision energy of 0.2 eV).

4.2.2. Origin of size-dependent reactivity

As mentioned above, no reaction occurs between Co_mNO^+ ($m \leq 3$) and NO, probably because of shortage of the adsorption sites. Our previous study [9] has shown that NO is chemisorbed dissociatively onto the bridge sites of the triangular Co_3^+. The second NO molecule may be adsorbed molecularly on Co_3NO^+, but it is desorbed immediately.

The size-dependency of the cross sections for the reaction, $Co_mNO^+ + NO$, in the $m \geq 4$ range is explained in terms of a picture that the size-dependency arises from the geometrical structure of the common intermediate species, $Co_m(N)_2(O)_2^+$. As described below, $Co_{m-x}(N)_2(O)_2^+$, is produced in the $m \geq 7$ range, while the energetics do not allow the production in the $m \leq 6$ range. It is likely that the N and O atoms in $Co_m(N)_2(O)_2^+$ occupy the bridge or the three-fold hollow sites of Co_m^+. If the cluster size is small enough, all of the Co atoms in the cluster are bonded to any of N or O atoms. In such a case, a large dissociation energy is needed to release one Co atom from the intermediate species. On the other hand, if the cluster size is large enough, not all of the Co atoms are occupied by N or O atoms, and the bond dissociation energy for the release of such naked Co atom(s) must be relatively small. Therefore, the release of the Co atom(s) (Eq. (10)) proceeds only in larger clusters.

A DFT calculation was performed for geometry optimization of the reactants, the intermediates, and the products at $m = 5$–7 in order to examine the validity of the picture mentioned above. The procedure for the geometry optimization was similar to that employed in the previous study [9]. In short, the DFT calculation was performed at a generalized-gradient-approximation (GGA) level on the ADF (Amsterdam Density Functional) program package [24]. The triple-zeta basis sets extended with a polarization function were employed for all the atoms involved. The frozen core approximation was applied for the 1s–2p orbitals of the Co atoms and the 1s orbital of the N and O atoms. The exchange-correlation terms adopted in the local-density-approximation (LDA) were those of Vosko et al. [25] and the exchange and the correlation functionals adopted for the GGA corrections were

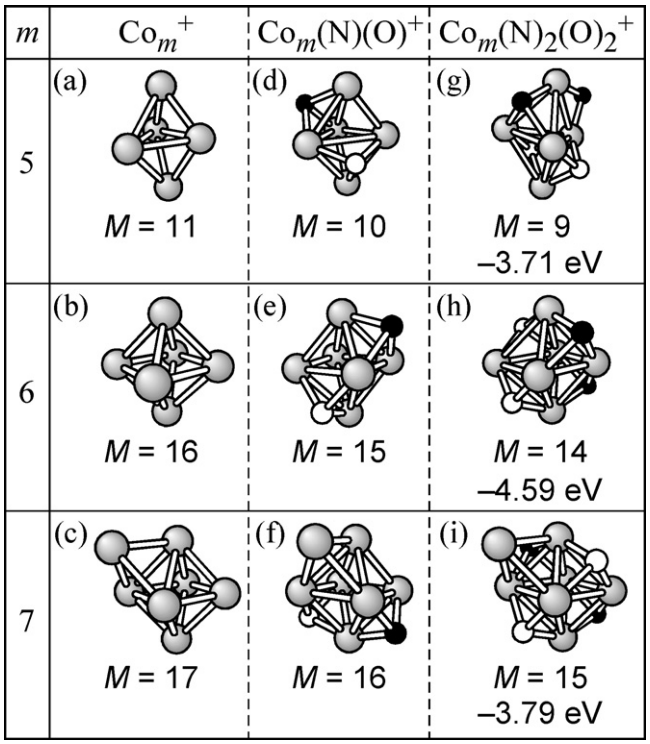

Fig. 6. Optimized geometries of Co_m^+ [(a)–(c)], $Co_m(N)(O)^+$ [(d)–(f)], and $Co_m(N)_2(O)_2^+$ [(g)–(i)] for $m = 5$–7 obtained by a DFT calculation are shown with the spin multiplicity, M ($=2S+1$). Gray, open, and solid circles represent Co, N, and O atoms, respectively. The number given under $Co_m(N)_2(O)_2^+$ shows its energy with respect to the energy of the initial state, $Co_m(N)(O)^+ + NO$.

those of Becke [26] and Perdew [27], respectively. The spin conservation rule was taken into account, and the intermediates and the products having the possible spin multiplicities were examined.

Fig. 6(a)–(c) shows the optimized geometries of the intact Co_m^+ in the ground states thus calculated. The initial geometries of the Co_mNO^+ were constructed by adding NO both molecularly and dissociatively on likely sites of Co_m^+, and the optimized geometries having the lowest energies were obtained. The dissociatively chemisorbed species, $Co_m(N)(O)^+$, illustrated in Fig. 6(d)–(f) was found to have the lowest energy. Similarly, the initial geometries for $Co_mN_2O_2^+$ were constructed by adding molecular and dissociative

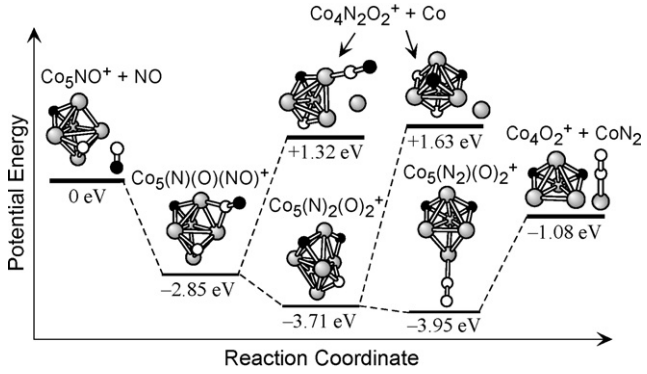

Fig. 7. Potential energy diagram for the reactions of Co_5NO^+ with NO is given with the optimized geometries of the reactants, intermediates, and product species, where gray, open, and solid circles represent Co, N, and O atoms, respectively. The numbers show the energies of the species with respect to the energy of the initial reaction state, $Co_5NO^+ + NO$.

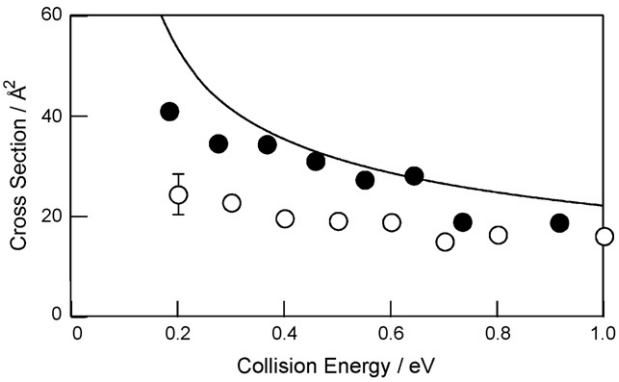

Fig. 8. Reaction cross sections for the NO decomposition of Co_5NO^+ (●) and Co_6NO^+ (○) with NO as a function of the collision energy. Only the NO decomposition was observed at the collision energies studied. The error bar gives one-standard deviation of the statistical errors. The solid line shows the collision-energy dependence of the Langevin cross section modified by taking the spread of the experimental collision energy into account.

NO to $Co_m(N)(O)^+$, and the lowest-energy structures obtained are shown in Fig. 6(g)–(i). The most stable geometries were found to be expressed as $Co_m(N)_2(O)_2^+$ in which the second NO molecules are dissociated and atomically adsorbed on the three-fold hollow and bridge sites of Co_m^+. It should be emphasized that every Co atom in $Co_m(N)_2(O)_2^+$ at $m = 5$ or 6 takes part in the adsorption of the N or O atoms, while one Co atom in $Co_7(N)_2(O)_2^+$ is naked. The bond dissociation energy of the naked Co atom in $Co_7(N)_2(O)_2^+$ was estimated to be 3.45 eV, and those of a bonded Co atom in $Co_m(N)_2(O)_2^+$ at $m = 5$ and 6 were 5.34 and 4.92 eV, respectively. Here, the bond dissociation energy was calculated as the energy difference of the optimized $Co_m(N)_2(O)_2^+$ and $Co_{m-1}(N)_2(O)_2^+ + Co$. As expected, the dissociation energy is relatively small at $m = 7$ where a bare Co atom, which is bound only to other Co atoms, is released, while the dissociation energy is larger at $m = 5$ and 6 where the leaving Co atom has to break the bond to any of the N or O atoms. In conclusion, the present calculation supports the picture that (1) the chemisorption of two NO occurs in the $m \geq 7$ range because the intermediate species, $Co_m(N)_2(O)_2^+$, is stabilized by the release of a bare Co, and (2) any Co atom is not released from $Co_m(N)_2(O)_2^+$ at $m \leq 6$ because all the Co atoms in $Co_m(N)_2(O)_2^+$ are bound to any of the N or O atoms and the bond dissociation energy of a Co atom is relatively large.

Fig. 7 summarizes the calculated energy diagram of Co_5NO^+ with NO. The energies of the intermediates and the products are given with respect to the initial state, $Co_5NO^+ + NO$. We found three reaction intermediates, $Co_5(N)(O)(NO)^+$, $Co_5(N)_2(O)_2^+$, and $Co_5(N_2)(O)_2^+$, which have lower energies than that of the initial state. The second NO molecule is adsorbed molecularly, and then, dissociates into the molecule-like nitrogen on the cluster. The final product state, $Co_4(O)_2^+ + CoN_2$, in the NO dissociation process is also energetically more stable than that of the initial state. Although the transition states were not calculated here, this calculation indicates that the NO dissociation reaction is exothermic and can easily proceed at $m = 5$, on the premise that there is no appreciable energy barrier along the reaction coordinate. This finding is consistent with the experimental observations. On the other hand, the calculation shows that a Co atom release from either intermediate, $Co_5(N)(O)(NO)^+$ or $Co_5(N)_2(O)_2^+$, is endothermic because of the large bond dissociation energy of the Co atom. In conclusion, the size-dependency originates from the energetics of the reactions involved; the NO decomposition occurs on a smaller cluster, and the chemisorption with the Co atom release occurs only on a larger cluster.

4.2.3. Energy barrier in NO decomposition process

Let us focus on the cross sections of the NO decomposition from Co_mNO^+ (m = 4–6) (see Fig. 5). The reaction cross section of Co_5NO^+ is comparative to the Langevin cross section (the upper limit of the collision cross section) while that of $Co_{4,6}NO^+$ is about a half of the Langevin cross section at the collision energy of 0.2 eV. This is explained by assuming a higher energy barrier along the reaction coordinate of the NO decomposition; the reaction cross section is small if the reaction intermediates cannot surmount the energy barrier efficiently. This assumption is supported by the collision-energy dependence of the reaction cross section shown in Fig. 8. The reaction cross section of Co_5NO^+ is comparable to the Langevin cross section at the collision energies larger than 0.2 eV. On the other hand, the reaction cross section of Co_6NO^+ gradually approaches to the Langevin cross section as the collision energy increases. This result is consistent with the existence of the energy barrier because the energy barrier is more efficiently surmounted when a larger available energy is introduced by the collision.

5. Conclusions

In the present study, we investigated the reactions of Co_n^+ with NO molecules under the multiple collision conditions, and showed that the NO decomposition and the chemisorption of two NO are major reactions through double collisions of NO onto Co_n^+, in which the reaction intermediate species, $Co_{n-1}NO^+$, is going to the products in collision with the second NO. Size-dependent reactivity is controlled by the bond dissociation energy of the intermediate species. This picture is consistent with the FT-ICR study of Mackenzie and co-workers (see footnote 3).

Acknowledgements

We are pleased to dedicate this paper to Professor Zdenek Herman on the occasion of his 75th birthday. This work was supported by the Special Cluster Research Project of Genesis Research Institute, Inc.

References

[1] M. Che, C.O. Bennett, Adv. Catal. 36 (1989) 55.
[2] C.R. Henry, Surf. Sci. Rep. 31 (1998) 231.
[3] A.W. Castleman Jr., P. Jena, Proc. Natl. Acad. Sci. USA 103 (2006) 10552.
[4] M.B. Knickelbein, Annu. Rev. Phys. Chem. 50 (1999) 79.
[5] P.B. Armentrout, Annu. Rev. Phys. Chem. 52 (2001) 423.
[6] K.A. Zemski, D.R. Justes, A.W. Castleman Jr., J. Phys. Chem. B 106 (2002) 6136.
[7] K.M. Ervin, Int. Rev. Phys. Chem. 20 (2001) 127.
[8] P. Warneck, Chemistry of the Natural Atmosphere, Academic Press, San Diego, 1988.
[9] T. Hanmura, M. Ichihashi, Y. Watanabe, N. Isomura, T. Kondow, J. Phys. Chem. A 111 (2007) 422.
[10] W.D. Vann, R.C. Bell, A.W. Castleman Jr., J. Phys. Chem. A 103 (1999) 10846.
[11] Q. Wu, S. Yang, Int. J. Mass Spectrom. 184 (1999) 57.
[12] M.S. Ford, M.L. Anderson, M.P. Barrow, D.P. Woodruff, T. Drewello, P.J. Derrick, S.R. Mackenzie, Phys. Chem. Chem. Phys. 7 (2005) 975.
[13] M.L. Anderson, M.S. Ford, P.J. Derrick, T. Drewello, D.P. Woodruff, S.R. Mackenzie, J. Phys. Chem. A 110 (2006) 10992.
[14] M. Iwamoto, H. Hamada, Catal. Today 10 (1991) 57.
[15] V.I. Pârvulescu, P. Grange, B. Delmon, Catal. Today 46 (1998) 233.
[16] J.J. Klaassen, D.B. Jacobson, J. Am. Chem. Soc. 110 (1988) 974.
[17] J.J. Klaassen, D.B. Jacobson, Inorg. Chem. 28 (1989) 2022.
[18] A. Martinez, C. Jamorski, G. Medina, D.R. Salahub, J. Phys. Chem. A 102 (1998) 4643.
[19] T. Hanmura, M. Ichihashi, T. Kondow, Israel J. Chem. 47 (2007) 37.
[20] J. Hirokawa, M. Ichihashi, S. Nonose, T. Tahara, T. Nagata, T. Kondow, J. Chem. Phys. 101 (1994) 6625.
[21] M. Ichihashi, T. Hanmura, R.T. Yadav, T. Kondow, J. Phys. Chem. A 104 (2000) 11885.
[22] R.D. Levine, R.B. Bernstein, Molecular Reaction Dynamics, Oxford University Press, Oxford, 1974.
[23] J. Pilme, B. Silvi, M.E. Alikhani, J. Phys. Chem. A 109 (2005) 10028.
[24] (a) ADF 2003.01, SCM, Theoretical Chemistry, Vrije Universiteit, Amsterdam, The Netherlands, http://www.scm.com;
(b) G. te Velde, F.M. Bickelhaupt, S.J.A. van Gisbergen, C. Fonseca Guerra, E.J. Baerends, J.G. Snijders, T. Ziegler, J. Comput. Chem. 22 (2001) 931;
(c) C. Fonseca Guerra, J.G. Snijders, G. te Velde, E.J. Baerends, Theor. Chem. Acc. 99 (1998) 391.
[25] S.H. Vosko, L. Wilk, M. Nusair, Can. J. Phys. 58 (1980) 1200.
[26] A.D. Becke, Phys. Rev. A 38 (1988) 3098.
[27] J.P. Perdew, Phys. Rev. B 33 (1986) 8822.